Published for SISSA by Springer

Received: *April 18, 2024*
Revised: *May 16, 2024*
Accepted: *May 22, 2024*
Published: *June 18, 2024*

Skyrmion crystals stabilized by ω-mesons

Derek Harland,[a] **Paul Leask**[a,b] **and Martin Speight**[a]

[a]*School of Mathematics, University of Leeds, Leeds, LS2 9JT, England, U.K.*
[b]*Department of Physics, KTH Royal Institute of Technology, 10691 Stockholm, Sweden*

E-mail: d.g.harland@leeds.ac.uk, palea@kth.se, j.m.speight@leeds.ac.uk

Abstract: We investigate the ground state crystalline structure of nuclear matter in the ω-meson variant of the Skyrme model. After minimizing energy with respect to variations of both the Skyrme field and the period lattice, we find four distinct periodic solutions which are similar to those found in the standard Skyrme model. We use these crystals to calculate coefficients in the Bethe-Weizsäcker semi-empirical mass formula and the compression modulus of infinite nuclear matter, and find a significant improvement as compared with other variants of the Skyrme model.

Keywords: Solitons Monopoles and Instantons, Differential and Algebraic Geometry, Field Theories in Lower Dimensions, Topological States of Matter

ArXiv ePrint: 2404.11287

Open Access, © The Authors.
Article funded by SCOAP^3.

https://doi.org/10.1007/JHEP06(2024)116

JHEP06(2024)116

Contents

1 Introduction

Skyrme models are a class of chiral Lagrangians in which baryons are modeled using topological solitons. In common with all chiral Lagrangians, they can be considered low-energy descriptions of quantum chromodynamics (QCD). The identification of solitons with baryons is justified by Witten's observation that the baryon number $B \in \mathbb{Z}$ can be identified with the degree of the chiral field $\varphi : \mathbb{R}^3 \to \mathrm{SU}(2)$ [1, 2].

The simplest chiral Lagrangian, consisting of a nonlinear sigma model and a pion mass term, does not support stable solitons, so additional terms must be included in the Lagrangian in order to stabilize them. Skyrme's proposal was the inclusion of a higher fourth-order term with opposing scaling behavior to provide the soliton with a scale [3]. This is known as the standard Skyrme model, and it is widely studied as a model of atomic nuclei and dense nuclear matter.

Dense nuclear matter can be modeled in the standard Skyrme model using crystals [4]. These are periodic solutions of the Euler-Lagrange equations that minimize the energy per unit cell. In the model with massless pions, the crystal with the lowest energy per baryon number was discovered independently by Kugler and Shtrikman [5] and Castillejo et al. [6]. This crystal resembles a cubic lattice, with each vertex carrying baryon number 1/2, and is referred to as a lattice of half-skyrmions, or the $\mathrm{SC}_{1/2}$ crystal. Crystals in the model with non-zero pion mass have been investigated recently [7]. The pion mass breaks chiral symmetry, and as a result the $\mathrm{SC}_{1/2}$ crystal degenerates to four distinct crystals with slightly different energies. Two of these crystals, including the one with the lowest energy, do not enjoy cubic lattice symmetry and their fundamental domains are cuboidal but not cubic. The discovery of these non-cubic crystals was enabled by a new energy-minimization algorithm that allows the lattice structure, as well as the Skyrme field, to vary.

This paper concerns a variant of the Skyrme model that was first proposed by Adkins and Nappi [8]. This model does not include a Skyrme term; instead, solitons are stabilized

JHEP06(2024)116

by an ω-meson field that is coupled anomalously to the chiral field φ through the Wess-Zumino term. While it is well-motivated, this model initially received less attention than the standard Skyrme model because it has proved much harder to find soliton solutions. The technical reason for this is that the energy is not bounded from below, rendering gradient descent-based energy minimization algorithms useless. Interest in the model was revived in [9], which constructed the first topological solitons with $B > 1$, albeit within the rational map approximation. Progress has also been made in the $B = 1$ sector [10], where it was shown that a simple perturbation of the model can reproduce the neutron-proton mass difference.

In a recent paper [11] a new method for constructing solitons in this model was developed. Therein, they found true static solutions for topological charges 1 through 8, for a range of coupling constants. Suitably calibrated, the model reproduces several properties of atomic nuclei with reasonable accuracy. In particular, its classical binding energies are comparable with experimental values, which is not the case in the standard Skyrme model. With this calibration the shapes of solitons are sometimes different from the standard Skyrme model, and from the predictions of the rational map approximation.

This paper presents an investigation of crystals in the ω-meson Skyrme model, using the methods of [7] and [11]. As in the standard Skyrme model, we find four distinct crystals, and the crystal with the lowest energy differs from the crystal of [5, 6] both in its iso-orientation and its symmetries. From these crystals we are able to calculate coefficients in the Bethe-Weizsäcker semi-empirical mass formula and the nuclear matter incompressibility coefficient. In both cases we obtain more acceptable values than had been obtained in other Skyrme models. Furthermore, the method developed herein has also been utilized to determine crystals in the baby Skyrme model coupled to the ω-meson [12].

Skyrmion crystals involving vector mesons have been studied elsewhere in the literature, for example in [13, 14]. These papers did not use the Adkins-Nappi model considered here but instead investigated more complicated Skyrme models: the model in [13] included ρ-mesons and scalar fields in addition to the pion and ω fields, while the model in [14] was based on the entirely different framework of hidden local symmetry (HLS) and holography. In the HLS approach, the hidden symmetry of the nonlinear σ model is gauged and the corresponding gauge particle acquires mass through the Higgs mechanism [15]. This allows for the incorporation of ρ-mesons, as well as the ω-meson. Nevertheless, in both of these papers, the Kugler-Shtrikman Fourier series method [5] was generalized to incorporate vector mesons. This method assumed a cubic lattice symmetry from the outset and did not allow the lattice geometry to vary, so it is was not able to find the new lower-energy crystals discovered in this paper. The recent paper [16] constructs exact solutions to the Adkins-Nappi model on compact domains. However, unlike the crystals studied here, these solutions are time-dependent. When extended periodically, the solutions of [16] have zero baryon number per unit period, whereas our skyrmion crystals have non-zero baryon number per unit period.

The ω-meson model is presented in the next section, where we also present a new topological energy bound valid for crystals and, more generally, for skyrmions on compact domains. In section 3 we present our energy-minimization algorithm and compute the relevant stress-energy tensor. We present our new crystal solutions in sections 4, and proceed to calculate the semi-empirical mass formula and nuclear matter incompressibility coefficient in sections 5 and 6. We draw conclusions in section 7.

JHEP06(2024)116

2 The ω-Skyrme model

The ω-meson variant of the Skyrme model is a non-linear sigma model coupled to the isoscalar ω vector meson field. It consists of the Skyrme field $\phi : \mathbb{R}^{1,3} \to \mathrm{SU}(2)$ and the ω vector meson, which is a 1-form on $\mathbb{R}^{1,3}$. Here $\mathbb{R}^{1,3} = \mathbb{R} \times \mathbb{R}^3$ is Minkowski space with metric η and metric signature $+ - - -$. The ω-Skyrme Lagrangian defined by Adkins & Nappi [8] is given by

$$\mathcal{L} = \mathcal{L}_\phi + \mathcal{L}_\omega + \mathcal{L}_{\mathrm{WZ}}. \tag{2.1}$$

Here $\mathcal{L}_\phi$ is the sigma model Lagrangian with the explicit chiral symmetry breaking pion mass term,

$$\mathcal{L}_\phi = -\frac{F_\pi^2 m_\pi^2}{8\hbar^3} \operatorname{Tr}(\mathrm{Id}_2 - \phi) - \frac{F_\pi^2}{16\hbar} \eta^{\mu\nu} \operatorname{Tr}(L_\mu L_\nu), \quad L_\mu = \phi^\dagger \partial_\mu \phi. \tag{2.2}$$

The minimally broken $\mathrm{U}(1)_V$ Lagrangian for spin-1 mesons is given by the term

$$\mathcal{L}_\omega = \frac{m_\omega^2}{2\hbar^3} \eta^{\mu\nu} \omega_\mu \omega_\nu - \frac{1}{4\hbar} \eta^{\mu\alpha} \eta^{\nu\beta} \omega_{\mu\nu} \omega_{\alpha\beta}, \quad \omega_{\mu\nu} = \partial_\mu \omega_\nu - \partial_\nu \omega_\mu, \tag{2.3}$$

and the gauged Wess-Zumino term is

$$\mathcal{L}_{\mathrm{WZ}} = \beta_\omega \omega_\mu \mathcal{B}^\mu, \quad \mathcal{B}^\mu = \frac{1}{24\pi^2\sqrt{-\eta}} \epsilon^{\mu\nu\rho\sigma} \operatorname{Tr}(L_\nu L_\rho L_\sigma), \tag{2.4}$$

which describes the coupling of the ω-meson to three pions. The baryon number can be identified with a topological charge and is given by

$$B = \int_{\mathbb{R}^3} \mathrm{d}^3x \sqrt{-\eta}\, \mathcal{B}^0. \tag{2.5}$$

The main free parameters of this model are the pion decay constant F_π, the pion mass m_π, the ω-meson mass m_ω, and the coupling constant β_ω, while $\hbar = 197.3\,\mathrm{MeV\,fm}$ is the reduced Planck constant. The coupling constant β_ω can be related to the $\omega \to \pi^+\pi^-\pi^0$ decay rate, which is in reality enhanced by the resonance $\omega \to \rho + \pi$, but is not included in the current theory. The decay rate, calculated using fiducial experimental values, is found to be $\Gamma_{\omega\to 3\pi} = 8.49\,\mathrm{MeV}$, which gives the upper bound $\beta_\omega \leq 23.9$ [11].

For convenience, we follow Sutcliffe [9] and rescale the ω meson by $\omega \mapsto \omega F_\pi$, and choose the classical energy scale to be $\tilde{E} = F_\pi^2/m_\omega$ (MeV) and the length scale to be $\tilde{L} = \hbar/m_\omega$ (fm). Then the rescaled ω-Skyrme Lagrangian in dimensionless units is given by

$$\mathcal{L} = -\frac{m^2}{8} \operatorname{Tr}(\mathrm{Id}_2 - \phi) - \frac{1}{16} \eta^{\mu\nu} \operatorname{Tr}(L_\mu L_\nu) + \frac{1}{2} \eta^{\mu\nu} \omega_\mu \omega_\nu - \frac{1}{4} \eta^{\mu\alpha} \eta^{\nu\beta} \omega_{\mu\nu} \omega_{\alpha\beta} + c_\omega \omega_\mu \mathcal{B}^\mu, \tag{2.6}$$

where the rescaled pion mass and ω coupling constant are, respectively, $m = m_\pi/m_\omega$ and $c_\omega = m_\omega \beta_\omega / F_\pi$. The energy-momentum tensor (in dimensionless Skyrme units) is given by

$$\begin{aligned} T_{\mu\nu} &= \frac{2}{\sqrt{-\eta}} \frac{\partial(\sqrt{-\eta}\mathcal{L})}{\partial \eta^{\mu\nu}} = 2\frac{\partial \mathcal{L}}{\partial \eta^{\mu\nu}} - \eta_{\mu\nu}\mathcal{L} \\ &= -\frac{1}{8} \operatorname{Tr}(L_\mu L_\nu) + \omega_\mu \omega_\nu - \eta^{\alpha\beta} \omega_{\mu\alpha} \omega_{\nu\beta} - \eta_{\mu\nu} \left\{ -\frac{m^2}{8} \operatorname{Tr}(\mathrm{Id}_2 - \phi) \right. \\ &\quad \left. -\frac{1}{16} \eta^{\alpha\beta} \operatorname{Tr}(L_\alpha L_\beta) + \frac{1}{2} \eta^{\alpha\beta} \omega_\alpha \omega_\beta - \frac{1}{4} \eta^{\alpha\rho} \eta^{\beta\sigma} \omega_{\alpha\beta} \omega_{\rho\sigma} \right\}. \end{aligned} \tag{2.7}$$

JHEP06(2024)116

Notice that the Wess-Zumino Lagrangian makes no contribution to this because it does not depend on the metric tensor. The energy functional is obtained from the temporal part of the energy-momentum tensor. For the Minkowski metric this is

$$\mathcal{E} = \frac{m^2}{8}\operatorname{Tr}(\mathrm{Id}_2 - \phi) - \frac{1}{16}\operatorname{Tr}(L_iL_i + L_0L_0) + \frac{1}{2}\omega_0^2 + \frac{1}{2}\omega_i\omega_i + \frac{1}{2}\omega_{0i}\omega_{0i} + \frac{1}{4}\omega_{ij}\omega_{ij}. \tag{2.8}$$

We are only interested in finding static solutions, so we write $\phi(x,t) = \varphi(x)$, where the map $\varphi : \mathbb{R}^3 \to \mathrm{SU}(2)$ will now be identified as the Skyrme field. In particular, we will study this model on the physical space $\mathbb{R}^3$ under the assumption of periodicity with respect to some 3-dimensional lattice

$$\Lambda = \left\{ n_1\vec{X}_1 + n_2\vec{X}_2 + n_3\vec{X}_3 : n_i \in \mathbb{Z} \right\}. \tag{2.9}$$

We do so by interpreting the domain of the fields φ, ω as $\mathbb{R}^3/\Lambda$, where $(\mathbb{R}^3/\Lambda, d)$ is a 3-torus equipped with the standard Euclidean metric d. It will prove convenient to identify this domain with the unit 3-torus by $\mathbb{T}^3 \equiv S^1 \times S^1 \times S^1 = \mathbb{R}^3/\mathbb{Z}^3$ via the obvious diffeomorphism

$$F : \mathbb{T}^3 \to \mathbb{R}^3/\Lambda, \quad (x_1, x_2, x_3) \mapsto x_1\vec{X}_1 + x_2\vec{X}_2 + x_3\vec{X}_3. \tag{2.10}$$

The Euclidean metric d on $\mathbb{R}^3/\Lambda$ can be identified with the pullback metric g on $\mathbb{T}^3$, i.e.

$$g = F^*d = g_{ij}\mathrm{d}x_i\mathrm{d}x_j, \quad g_{ij} = \vec{X}_i \cdot \vec{X}_j. \tag{2.11}$$

Varying the lattice Λ is then equivalent to varying the flat metric g on T^3.

We will write the Skyrme field using pion field notation, that is, we write $\varphi = \varphi_0\,\mathrm{Id}_2 + i\varphi_j\tau^j$ where τ^j are the usual Pauli spin matrices. Then, we identify $\mathrm{SU}(2)$ with S^3 via the isometry

$$\mathrm{SU}(2) \ni \begin{pmatrix} \varphi_0 + i\varphi_3 & i\varphi_1 + \varphi_2 \\ i\varphi_1 - \varphi_2 & \varphi_0 - i\varphi_3 \end{pmatrix} \leftrightarrow (\varphi_0, \varphi_1, \varphi_2, \varphi_3) \in S^3. \tag{2.12}$$

The three fields $\varphi_1, \varphi_2, \varphi_3$ are identified with pions, and the field φ_0 is sometimes referred to as the σ-field and is constrained by the equation $\varphi_A\varphi_A = 1$, where the repeated index is summed over $A = 0, 1, 2, 3$.

Since we are only interested in static field configurations, only the temporal component of the topological current remains, i.e. $\mathcal{B}^i = 0$. Consequently, only the temporal component ω_0 of the ω-meson survives, since the topological charge density acts as a source term for the ω field. For notational convenience, we will drop the subscript and denote $\omega \equiv \omega_0$. With these conventions, the static Lagrangian and energy functionals obtained by integrating (2.6) and (2.8) over one period are

$$-L(\varphi, \omega, g) = \int_{\mathbb{T}^3} \mathrm{d}^3x\sqrt{g}\left\{ \frac{1}{4}m^2(1-\varphi_0) + \frac{1}{8}g^{ij}\partial_i\varphi_A\partial_j\varphi_A - \frac{1}{2}g^{ij}\partial_i\omega\partial_j\omega - \frac{1}{2}\omega^2 - c_\omega\omega\mathcal{B}_0 \right\}, \tag{2.13}$$

$$E(\varphi, \omega, g) = \int_{\mathbb{T}^3} \mathrm{d}^3x\sqrt{g}\left\{ \frac{1}{4}m^2(1-\varphi_0) + \frac{1}{8}g^{ij}\partial_i\varphi_A\partial_j\varphi_A + \frac{1}{2}g^{ij}\partial_i\omega\partial_j\omega + \frac{1}{2}\omega^2 \right\}. \tag{2.14}$$

Solutions of the Euler-Lagrange equations are critical points of the Lagrangian (2.13). Since this is not bounded from above or below it is not amenable to standard energy-minimisation

JHEP06(2024)116

methods. Following [11] we reformulate it using the Euler-Lagrange equation corresponding to temporal ω,

$$\left(-g^{ij}\partial_i\partial_j + 1\right)\omega = -c_\omega \mathcal{B}_0. \tag{2.15}$$

This is a linear equation for ω with a source term proportional to the baryon current. The ω-meson is completely determined by the Skyrme field φ and the domain metric g. Taking the inner product of (2.15) with ω and integrating by parts yields

$$\int_{\mathbb{T}^3} \mathrm{d}^3x\sqrt{g}\, c_\omega \omega \mathcal{B}_0 = -\int_{\mathbb{T}^3} \mathrm{d}^3x\sqrt{g}\, \left(g^{ij}\partial_i\omega\partial_j\omega + \omega^2\right). \tag{2.16}$$

It follows that $-L$ given (2.13) is equal to the energy (2.14) when ω satisfies the constraint (2.15). Extremising the unbounded functional (2.13) with respect to variations φ and ω is equivalent to extremising the bounded energy (2.14) subject to the constraint (2.15).

We wish to find skyrmion crystals, i.e. static periodic solutions φ, ω of the Euler-Lagrange equations whose energy is minimized with respect to variations of the period lattice Λ. We do so by minimizing (2.14) with respect to variations in φ, g, with ω being determined by the constraint (2.15). We will describe a numerical method for doing so in the next section.

Before moving on, it is interesting to note that the energy (2.14) subject the constraint (2.15) obeys a topological energy bound. In fact, the bound is valid in the more general setting of maps $\varphi : M \to N$ between compact Riemannian 3-manifolds (M^3, g) and (N^3, h), so we reformulate the energy in this more general setting. We have a functional given by

$$E(\varphi, g) = \int_M \left(\frac{1}{8}\left|\mathrm{d}\varphi\right|_g^2 + \frac{1}{4}(V\circ\varphi) + \frac{1}{2}\left|\mathrm{d}\omega\right|_g^2 + \frac{1}{2}\omega^2\right)\mathrm{vol}_g, \tag{2.17}$$

subject to the constraint

$$(\Delta_g + 1)\,\omega = -c_\omega * \varphi^*\Omega, \tag{2.18}$$

where Ω is the normalized volume form on N, i.e.

$$\Omega = \frac{\mathrm{vol}_h}{|N|}. \tag{2.19}$$

Proposition 2.1. *The energy* (2.17) *subject to the constraint* (2.18) *satisfies the topological energy bound,*

$$E \geq \frac{B^2 c_\omega^2}{2|M|}, \tag{2.20}$$

in which B is the topological charge (i.e. degree) of $\varphi : M \to N$ and $|M|$ is the volume of M.

Proof. Let us define $\mathcal{B} = *\varphi^*\Omega$ such that $\varphi^*\Omega = \mathcal{B}\,\mathrm{vol}_g$. Then, from the ω-meson constraint (2.18), the topological charge can be expressed as

$$B = \int_M \varphi^*\Omega = -\frac{1}{c_\omega}\int_M (\Delta_g + 1)\,\omega\,\mathrm{vol}_g = -\frac{1}{c_\omega}\int_M \omega\,\mathrm{vol}_g. \tag{2.21}$$

Using the Cauchy-Schwartz inequality, we obtain the following relation

$$B^2 = \frac{1}{c_\omega^2}\left(\int_M \omega\,\mathrm{vol}_g\right)^2 \leq \frac{1}{c_\omega^2}\left(\int_M \omega^2\,\mathrm{vol}_g\right)\left(\int_M 1\,\mathrm{vol}_g\right) = \frac{|M|}{c_\omega^2}\int_M \omega^2\,\mathrm{vol}_g. \tag{2.22}$$

JHEP06(2024)116

With this, we can derive a simple lower topological bound on the static energy (2.17), that is,

$$E \geq \frac{1}{2}\int_M \omega^2 \,\mathrm{vol}_g \geq \frac{B^2 c_\omega^2}{2|M|} \tag{2.23}$$

□

For the particular case of interest, $M = \mathbb{T}^3$ with flat metric given by a matrix g, the bound is

$$E \geq E_{\mathrm{bound}} = \frac{B^2 c_\omega^2}{2\sqrt{g}}. \tag{2.24}$$

3 Energy minimization and the stress-energy tensor

We now turn to the problem of constructing skyrmion crystals, i.e. minimizing the energy (2.14) with respect to variations in φ and g. We do this numerically, using arrested Newton flow. This algorithm works by solving Newton's equations of motion for the energy E, written formally as:

$$\frac{\mathrm{d}^2}{\mathrm{d}t^2}(\varphi_A, g_{ij}) = -\nabla E. \tag{3.1}$$

Initial conditions are chosen such that $\frac{\mathrm{d}}{\mathrm{d}t}(\varphi_A, g_{ij}) = 0$. These ensure that the flow reduces energy at early times. If at any later time the energy begins to increase, the flow is arrested and the velocities $\frac{\mathrm{d}}{\mathrm{d}t}(\varphi_A, g_{ij})$ are set to zero. The flow then resumes from the same position. It is deemed to have converged when ∇E is sufficiently small.

We recall that ω appearing in the energy functional (2.14) depends on φ and g through the constraint (2.15). Thus computing E and its gradient entails computing ω at each time step. As in [11], this is accomplished using a conjugate gradient method. The constraint (2.15) means that the metric-dependence of the energy is much more complicated than in the standard Skyrme model. As a result, the algorithm described here is slightly different from the algorithm used earlier to find crystals in the standard Skyrme model [7].

The gradient on the right hand side of (3.1) is understood using the calculus of variations. We write $\nabla E = (\Phi_A, S_{ij})$, in which Φ_A and S_{ij} are defined by

$$\frac{\mathrm{d}}{\mathrm{d}s}E(\varphi_s, g_s)\bigg|_{s=0} = \int_{\mathbb{T}^3} \mathrm{d}^3x\sqrt{g}\,\left(\Phi_A(\varphi, g)\dot{\varphi}_A + S_{ij}(\varphi, g)\dot{g}_{kl}g^{jk}g^{li}\right) \tag{3.2}$$

for all one-parameter variations φ_s, g_s with $(\varphi_0, g_0) = (\varphi, g)$ and $\frac{\mathrm{d}}{\mathrm{d}s}(\varphi_s, g_s) = (\dot{\varphi}, \dot{g})$ at $s = 0$. The calculation of Φ_A and S_{ij} is delicate, because ω appearing in (2.14) depends on φ and g implicitly through the constraint (2.15). Using results of [11], Φ_A is given (in the case of flat metrics on $\mathbb{T}^3$) by

$$\Phi_A = -\frac{1}{4}(\delta_{AB} - \varphi_A\varphi_B)(m^2\delta_{0B} + g^{ij}\partial_i\partial_j\varphi_B) + \frac{c_\omega}{4\pi^2\sqrt{g}}\epsilon_{ijk}\epsilon_{ABCD}\varphi_B\partial_i\omega\partial_j\varphi_C\partial_k\varphi_D, \tag{3.3}$$

where $A, B, C, D = 0, 1, 2, 3$. This coincides with the Euler-Lagrange equation of the original unconstrained energy functional (2.13). The stress-energy tensor S_{ij} is computed in the following proposition, formulated in the general setting of maps $\varphi : (M, g) \to (N, h)$ between Riemannian 3-manifolds.

JHEP06(2024)116

Proposition 3.1. *The stress-energy tensor* $S = S_{ij}\mathrm{d}x^i\mathrm{d}x^j$ *associated to the energy* (2.17) *subject to the constraint* (2.18) *is the section of* $\mathrm{Sym}^2(T^*M)$ *given by*

$$S(\varphi, g) = \left(\frac{1}{16}|\mathrm{d}\varphi|_g^2 + \frac{1}{8}(V\circ\varphi) - \frac{1}{4}|\mathrm{d}\omega|_g^2 - \frac{1}{4}\omega^2\right) g - \left(\frac{1}{8}\varphi^* h - \frac{1}{2}\mathrm{d}\omega\otimes\mathrm{d}\omega\right). \tag{3.4}$$

Note that in local coordinates the formula (3.4) gives

$$\begin{aligned} S_{ij} = &\left(\frac{1}{16}g^{mn}\partial_m\varphi_A\partial_n\varphi_A + \frac{1}{8}m^2\left(1-\varphi_0\right) - \frac{1}{4}g^{mn}\partial_m\omega\partial_n\omega - \frac{1}{4}\omega^2\right) g_{ij} \\ &- \frac{1}{8}\partial_i\varphi_A\partial_j\varphi_A + \frac{1}{2}\partial_i\omega\partial_j\omega. \end{aligned} \tag{3.5}$$

This coincides with the stress tensor for the original unconstrained energy functional (2.13).

Proof. Let us introduce the notation $\langle A, B\rangle_g = A_{ij}B_{kl}g^{ik}g^{jl}$ for the natural inner product of two-tensors $A = A_{ij}\mathrm{d}x^i\mathrm{d}x^j$, $B = B_{kl}\mathrm{d}x^k\mathrm{d}x^l$. The variation of the inverse metric and the volume form are given by

$$\left.\frac{\mathrm{d}}{\mathrm{d}s}\right|_{s=0} g^{ij}(s) = -g^{ik}\dot{g}_{kl}g^{lj}, \quad \left.\frac{\mathrm{d}}{\mathrm{d}s}\right|_{s=0}\mathrm{vol}_{g_s} = \frac{1}{2}\langle g, \dot{g}\rangle_g \mathrm{vol}_g. \tag{3.6}$$

These lead to the standard result for the first variation of the terms in (2.17) involving φ:

$$\frac{d}{ds}\int_M \left(\frac{1}{8}\left|\mathrm{d}\varphi\right|_g^2 + \frac{1}{4}(V\circ\varphi)\right)\mathrm{vol}_g\Big|_{s=0} = \int_M \left\langle \frac{1}{16}|\mathrm{d}\varphi|_g^2 g + \frac{1}{4}(V\circ\varphi)g - \frac{1}{8}\varphi^* h\,,\, \dot{g}\right\rangle_g \mathrm{vol}_g. \tag{3.7}$$

It remains to compute the first variation of the terms in (2.17) involving ω, which are more conveniently written using the constraint (2.18):

$$E^\omega(\omega, g) = \int_M \left(\frac{1}{2}\left|\mathrm{d}\omega\right|_g^2 + \frac{1}{2}\omega^2\right)\mathrm{vol}_g = -\frac{c_\omega}{2}\int_M \omega\varphi^*\Omega. \tag{3.8}$$

Since the pullback $\varphi^*\Omega \in \Omega^3(M)$ is g-independent, the first variation of this with respect to the metric g_s is given by

$$\left.\frac{\mathrm{d}E^\omega(\omega_s, g_s)}{\mathrm{d}s}\right|_{s=0} = -\frac{c_\omega}{2}\int_M \dot{\omega}\varphi^*\Omega = \frac{1}{2}\int_M \dot{\omega}\left(\Delta_g + 1\right)\omega\,\mathrm{vol}_g = \frac{1}{2}\int_M \omega\left(\Delta_g + 1\right)\dot{\omega}\,\mathrm{vol}_g, \tag{3.9}$$

where we have denoted $\dot{\omega} = \left.\frac{\mathrm{d}}{\mathrm{d}s}\right|_{s=0}\omega_s$. This can be simplified as follows. Consider the variation of the Hodge star operator $*_g : \Omega^3(M) \to \Omega^0(M)$,

$$\left.\frac{\mathrm{d}}{\mathrm{d}s}\right|_{s=0} *_{g_s} = -\frac{1}{2}\langle g, \dot{g}\rangle_g *_g, \tag{3.10}$$

and define $\dot{\Delta}_g = \left.\frac{\mathrm{d}}{\mathrm{d}s}\right|_{s=0}\Delta_{g_s}$. Then varying the ω-meson constraint (2.18) and using (3.10) yields

$$\left(\Delta_g + 1\right)\dot{\omega} = -\dot{\Delta}_g\omega + \frac{c_\omega}{2}\langle g, \dot{g}\rangle_g *_g \varphi^*\Omega \tag{3.11}$$

Hence the first variation (3.9) becomes

$$\left.\frac{\mathrm{d}E^\omega(\omega_s, g_s)}{\mathrm{d}s}\right|_{s=0} = \frac{c_\omega}{4}\int_M \langle g, \dot{g}\rangle_g \omega\,\phi^*\Omega - \frac{1}{2}\int_M \omega\dot{\Delta}_g\omega\,\mathrm{vol}_g. \tag{3.12}$$

JHEP06(2024)116

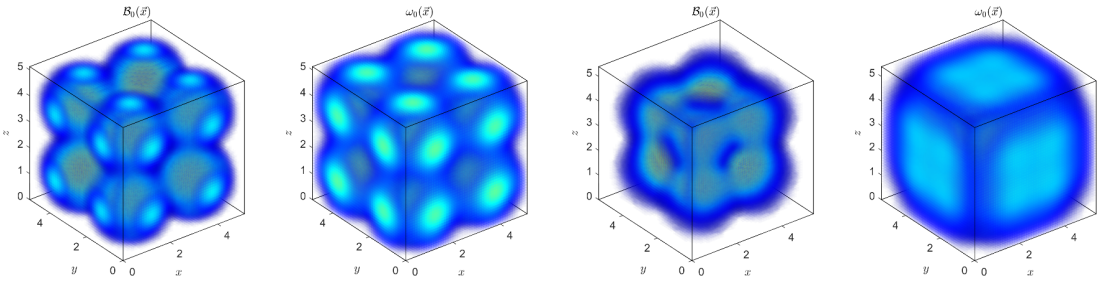

(a) $SC_{1/2}$ crystal. (b) α crystal.

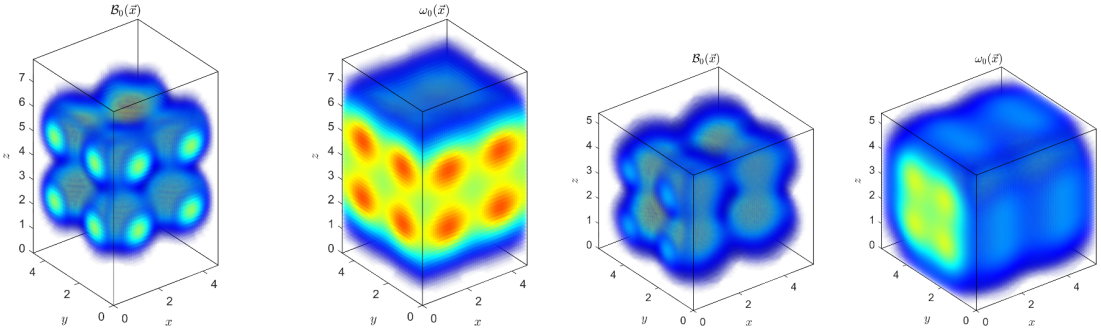

(c) multiwall crystal. (d) chain crystal.

Figure 1. Baryon density $\mathcal{B}_0(\vec{x})$ and omega density $\omega_0(\vec{x})$ plots of the four crystalline solutions for the coupling constant $c_\omega = 14.34$.

To simplify the second term, we vary the identity,

$$\int_M f(\Delta_{g_s} f)\mathrm{vol}_{g_s} = \int_M \langle \mathrm{d}f, \mathrm{d}f\rangle_{g_s}\,\mathrm{vol}_{g_s}, \tag{3.13}$$

to obtain

$$\int_M \left\{ f\dot{\Delta}_g f + \frac{1}{2} f(\Delta_g f)\langle g, \dot{g}\rangle_g \right\} \mathrm{vol}_g = \int_M \left\{ -\langle \mathrm{d}f \otimes \mathrm{d}f, \dot{g}\rangle_g + \frac{1}{2}|\mathrm{d}f|_g^2 \langle g, \dot{g}\rangle_g \right\} \mathrm{vol}_g, \tag{3.14}$$

valid for all smooth functions f. Using particular case $f = \omega$ of (3.14) and the constraint (2.18), (3.12) rearranges to

$$\left.\frac{\mathrm{d}E^\omega(\omega_s, g_s)}{\mathrm{d}s}\right|_{s=0} = \int_M \left\langle \frac{1}{2}\mathrm{d}\omega \otimes \mathrm{d}\omega - \frac{1}{4}|\mathrm{d}\omega|_g^2 g - \frac{1}{4}\omega^2 g\,,\, \dot{g} \right\rangle_g \mathrm{vol}_g. \tag{3.15}$$

Combining this with (3.7), the variation of E takes the form $\int_M \langle S, \dot{g}\rangle_g \mathrm{vol}_g$, with S given in (3.4). □

4 Skyrmion crystals coupled to ω-mesons

The previous sections have described our numerical algorithm that constructs skyrmion crystals by relaxing a choice of initial configuration. We now present the crystals obtained using this algorithm. As in [7], our initial configurations are based on the $SC_{1/2}$ crystal in

JHEP06(2024)116

the standard Skyrme model with no pion mass and no ω-mesons. We use the approximate solution $\varphi^{\text{app.}}$ of Castillejo et al. [6],

$$\varphi_0^{\text{app.}} = -c_1c_2c_3, \qquad \varphi_1^{\text{app.}} = s_1\sqrt{1-\frac{s_2^2}{2}-\frac{s_3^2}{2}+\frac{s_2^2s_3^2}{3}}, \tag{4.1}$$

with $s_i = \sin 2\pi x_i$, $c_i = \cos 2\pi x_i$, and $\varphi_2^{\text{app.}}, \varphi_3^{\text{app.}}$ obtained by cyclic permutation. This defines a Skyrme field on $\mathbb{R}^3/\mathbb{Z}^3$ with $B = 4$. As in [7], we generate a range of initial conditions $Q\varphi^{\text{app.}}$ using an SO(4) matrix Q. The four specific choices that we make for Q are:

$$\begin{aligned} Q_{1/2} &= \text{Id}, & Q_\alpha &= \frac{1}{\sqrt{3}}\begin{pmatrix} 0 & 1 & 1 & 1 \\ & & * & \end{pmatrix} \\ Q_{\text{multiwall}} &= \begin{pmatrix} 0 & 0 & 0 & 1 \\ & & * & \end{pmatrix}, & Q_{\text{chain}} &= \frac{1}{\sqrt{2}}\begin{pmatrix} 0 & 0 & 1 & 1 \\ & & * & \end{pmatrix}, \end{aligned} \tag{4.2}$$

with the remaining rows (denoted by an asterisk) being determined by the Gram-Schmidt process. These choices are motivated by the principle of symmetric criticality [7]. The initial metric is given by $g_{ij} = L^2\delta_{ij}$ for suitably chosen L. Following [11], we set the initial configuration for the ω-meson to be $\omega = -c_\omega\mathcal{B}_0$. The resulting initial conditions are invariant under distinct subgroups of the symmetry group of the energy functional, so flow to distinct critical points.

The energy (2.14) and constraint (2.15) involve two dimensionless parameters: c_ω and m. We used three different parameter choices that have been proposed in the literature [8, 9, 11]. Adkins and Nappi [8] chose the value $c_\omega = 98.4$ by fitting the masses of the nucleon and the delta resonance. Sutcliffe [9] chose the value $c_\omega = 34.7$ by fitting the pion decay constant F_π and the mass of helium-4 to their experimental values. Finally, Gudnason and Speight [11] chose the value $c_\omega = 14.34$ motivated by a range of considerations. In all calibrations, the parameter $m = m_\pi/m_\omega$ is close to its experimental value 0.176. For more details, see table 1.

The results of our relaxation algorithm are given in table 1. Plots of the baryon density and ω field are shown in figure 1 for $c_\omega = 14.34$ (pictures for other calibrations are similar). The 1/2 crystal always has a higher energy than the other three, but the α, chain, and multiwall crystals are very close in energy and their relative ordering might depend on c_ω. For $c_\omega = 14.34$ and 98.4 the multiwall crystal appears to have the lowest energy. For $c_\omega = 34.7$ the chain crystal may have a lower energy, but the numerical values are too close to be confident of this. For comparison, in the Skyrme model with no ω meson the multiwall-crystal has lowest energy [7].

We have not explored how the crystal energies depend on the parameter m_π/m_ω, but insight into this can be gained from the standard Skyrme model. In the standard Skyrme model the crystal energies coalesce as m_π tends to 0, and when $m_\pi = 0$ all four are related by SO(4) chiral rotations. We expect similar behaviour in the omega-meson model.

As in [7], the fundamental domain of the lattice Λ is not cubic for the multiwall and chain crystals. For the multiwall crystal the two equal side lengths are shorter than the third side, while for the chain crystal they are longer.

Finally, we note that the energies of the crystals are all greater than the bound (2.24) derived in Proposition 2.1 by a factor of at least 3.5. This is unsurprising, as the derivation

JHEP06(2024)116

Crystal	c_ω	F_π (MeV)	m_π (MeV)	m_ω (MeV)	E	E_0 (MeV)	n_0 (fm^{-3})
$SC_{1/2}$	98.4	124.0	138.0	782.0	145.7761	716.6	0.128
α	98.4	124.0	138.0	782.0	145.4590	715.0	0.125
chain	98.4	124.0	138.0	782.0	145.4526	715.0	0.125
multiwall	98.4	124.0	138.0	782.0	145.4477	715.0	0.125
$SC_{1/2}$	34.7	186.0	138.0	782.0	77.8067	860.6	0.526
α	34.7	186.0	138.0	782.0	77.7126	859.6	0.526
multiwall	34.7	186.0	138.0	782.0	77.6870	859.3	0.515
chain	34.7	186.0	138.0	782.0	77.6758	859.1	0.513
$SC_{1/2}$	14.34	139.8	43.91	249.5	47.2632	925.6	0.060
chain	14.34	139.8	43.91	249.5	47.0900	922.2	0.052
α	14.34	139.8	43.91	249.5	47.0867	922.1	0.051
multiwall	14.34	139.8	43.91	249.5	46.8397	917.3	0.047

Table 1. Comparison of the four crystalline solutions for the three different sets of parameters ($c_\omega = 98.4$ [8], $c_\omega = 34.7$ [9] and $c_\omega = 14.34$ [11]).

of the bound ignores most terms in the energy. The discrepancy seems to be greater for the lowest-energy solutions; this is because the bound (2.24) depends on the volume of the lattice fundamental domain, and solutions with lower energy happen to have large volumes. We expect the bound (2.24) to be more effective when the size of the lattice fundamental domain is constrained to be small.

5 Bethe-Weizsäcker semi-empirical mass formula

In this section we use skyrmion crystals to estimate coefficients in the Bethe-Weizsäcker semi-empirical mass formula. This is an approximate formula for the binding energy of a nucleus with baryon number B and takes the form

$$E_b = a_V B - a_S B^{2/3} - a_C \frac{Z(Z-1)}{B^{1/3}} - a_A \frac{(N-Z)^2}{B} + \delta(N,Z). \tag{5.1}$$

Here Z is the number of protons and $N = B - Z$ the number of neutrons. We will focus just on the first two terms, which are associated with the volume and surface area of the nucleus. Typical empirically-determined values for their coefficients are $a_V = 15.7 - 16.0\,\text{MeV}$ and $a_S = 17.3 - 18.4\,\text{MeV}$ [17].

We estimate these coefficients using the α-crystal in the calibration of Gudnason-Speight [11]. Following [18], we model a $B = 4N^3$ skyrmion as a cubic arrangement of $B = 4$ skyrmions. This can be regarded as a chunk of the α-crystal. To a first approximation, its energy is $E = BE_{\text{crystal}}$, where $E_{\text{crystal}} = 922.1\,\text{MeV}$ is the energy per baryon number of the α-crystal determined in the previous section. To make a better approximation, we add on a term $6N^2 E_{\text{face}}$ representing the surface energy, in which E_{face} represents the surface energy of one face of one cubic $B = 4$ skyrmion. To calculate the binding energy, we subtract this from B times the classical energy E_1 of a 1-skyrmion. This leads to the formula,

$$E_b = (E_1 - E_{\text{crystal}})B - \frac{3}{\sqrt[3]{2}} E_{\text{face}} B^{2/3}, \tag{5.2}$$

from which we can read off the coefficients a_V and a_S.

JHEP06(2024)116

We calculated E_1 using a fully three-dimensional arrested Newton flow and obtained the value 937.7 MeV in agreement with [11]. Thus it remains to calculate E_{face}. We have done so using a method developed in [19]. We regard the cubic lattice of $B = 4$ skyrmions as vertical stack of horizontal layers, each layer being a square array of $B = 4$ skyrmions. A horizontal slab consisting of n layers is doubly-periodic and has charge $4n$ in its fundamental domain. The energy contained in a fundamental domain can be estimated as

$$4nE_{\text{crystal}} + 2E_{\text{face}}, \tag{5.3}$$

because there are n cubic $B = 4$ skyrmions and two exposed faces. On the other hand, for any given n, the energy can be calculated precisely using the same method as was used to calculate the energy of the Skyrme crystal, the only difference being that the domain is $\mathbb{R} \times \mathbb{T}^2$ rather than $\mathbb{T}^3$, and only the components of the metric associated with $\mathbb{T}^2$ need to be varied. We have constructed these doubly-periodic slabs for a range of values of n using our relaxation algorithm.

By comparing these numerically-determined energies with the approximate formula (5.3) using a trust region reflective algorithm we have estimated the coefficient E_{face} to be 7.8 MeV. Then by comparing equations (5.1) and (5.2) we obtain the coefficients,

$$a_V = E_1 - E_{\text{crystal}} = 15.6\,\text{MeV}, \quad a_S = \frac{3}{\sqrt[3]{2}} E_{\text{face}} = 18.6\,\text{MeV}. \tag{5.4}$$

The resulting energy per nucleon curve is plotted in figure 2. For comparison, we have also plotted the energy per nucleon for the three cubic skyrmions with $B = 4N^3$ and $N = 1, 2, 3$ which have been calculated using arrested Newton flow, with initial configuration constructed using the rational map and product approximations. These are all close to the fitted curve, confirming the validity of the approximate formula (5.2). We also remark that the α-particle clustering seen here matches the clustering structure of light nuclei, and was also observed in the Skyrme model coupled to ρ-mesons [20].

Our predicted values (5.4) are in close agreement with the empirically-determined values. They are also a substantial improvement on the values $a_V = 136\,\text{MeV}$, $a_S = 320\,\text{MeV}$ obtained in the standard Skyrme model with massless pions [18]. This is consistent with the observation made in [11] that including the ω-meson substantially improves predictions of classical binding energies.

The remaining coefficients in the semi-empirical mass formula (5.1) have been investigated using Skyrme models elsewhere. Ma et al. [21] investigated the Coulomb energy in the standard Skyrme model. They found that $a_C = 0.608\,\text{MeV}$, which is in excellent agreement with the experimentally determined value of $a_C = 0.625\,\text{MeV}$. The asymmetry coefficient a_A was calculated using the sextic Skyrme model in [22]. By relating this to the symmetry energy of nuclear matter the value $a_A = 23.8\,\text{MeV}$ was obtained, which agrees extremely well with the experimental value $a_A = 23.7\,\text{MeV}$. It would be interesting to calculate these coefficients also in the omega-meson model, but doing so is beyond the scope of this paper.

6 Incompressibility of nuclear matter

We have seen that the Skyrme crystal in the ω-meson model provides a reasonable model of binding energies of finite nuclei. In this section we turn our attention to properties of infinite nuclear matter.

JHEP06(2024)116

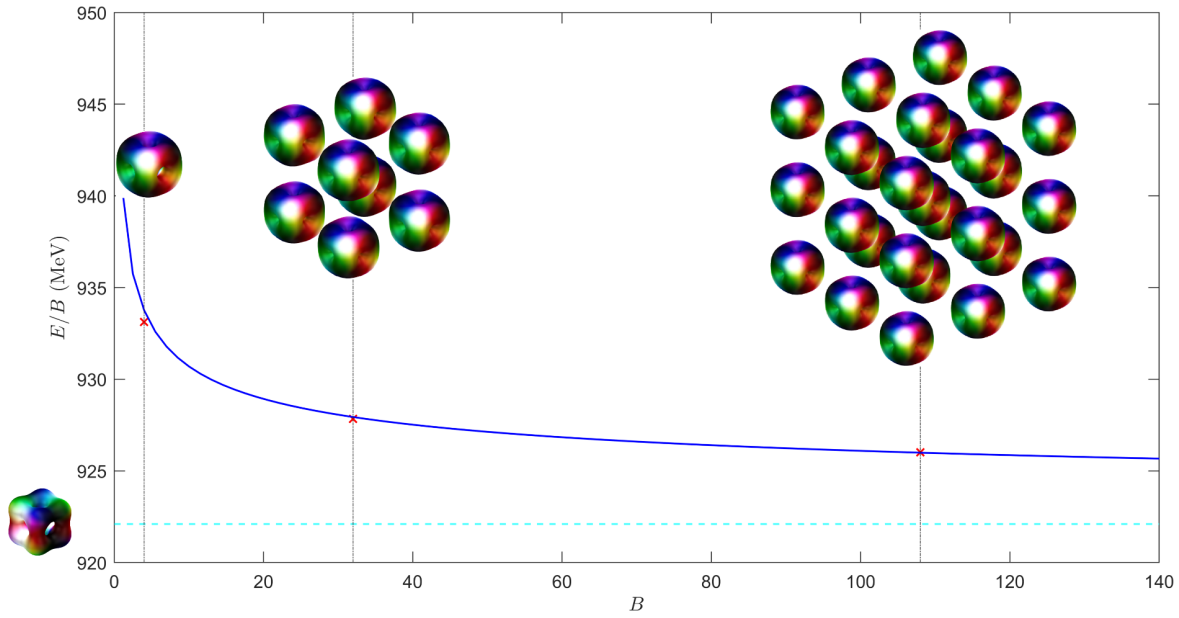

Figure 2. Plot of the Bethe-Weizsäcker SEMF from the α-particle approximation for the ω-Skyrme model.

Consider isospin symmetric nuclear matter at zero temperature, and let n_B be the baryon density, i.e. the number of protons and neutrons per unit volume. The (symmetric) energy per baryon of such matter can be approximated about the nuclear saturation density n_0 by use of a power series expansion [23]:

$$E(n_B)/B = E_0 + \frac{1}{2}K_0\frac{(n_B - n_0)^2}{9n_0^2} + \mathcal{O}\left((n_B - n_0)^3\right), \tag{6.1}$$

where the first term, associated to the nuclear saturation point n_0, is identified with the saturation energy $E_0 = E(n_0)/B$. The nuclear saturation density n_0 is defined to be the nuclear density such that $(\partial E)/(\partial n_B)|_{n_B=n_0} = 0$. There is no linear term since symmetric nuclear matter reaches a minimum of the energy at saturation. The next term is the one of interest, it is the nuclear incompressibility coefficient, or compression modulus, K_0, which can be obtained from the expansion (6.1),

$$K_0 = \frac{9n_0^2}{B}\frac{\partial^2 E}{\partial n_B^2}\bigg|_{n_0}. \tag{6.2}$$

This is a fundamental quantity in nuclear physics as it is a measure of nuclear resistance under pressure at the saturation point, and imposes significant constraints on the nuclear matter equation of state.

To compute the compression modulus in the Skyrme model, we need to construct skyrmion crystals with a range of baryon densities. In practice, we do this by minimizing the energy of the crystal with the volume of the fundamental cell of the lattice constrained to a constant value V. The baryon density of the resulting solution is $n_B = B/V$, with B being the baryon number per unit cell. The algorithm that we used to solve the constrained

JHEP06(2024)116

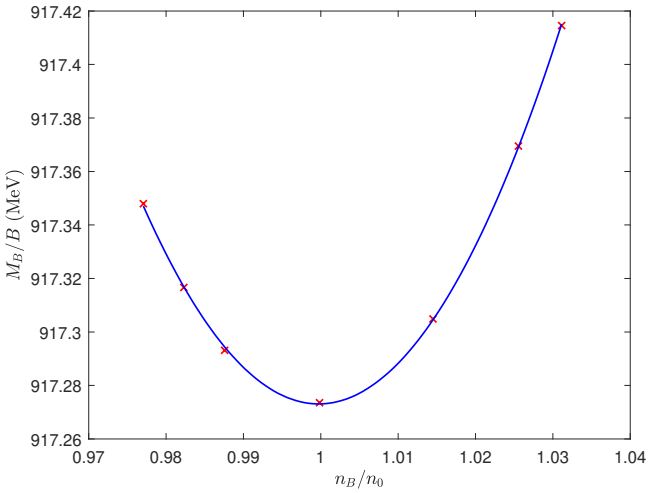

Figure 3. The energy per baryon E/B of the multi-wall crystal for various baryon densities n_B near saturation n_0.

energy-minimization problem is similar to the algorithm used for the unconstrained problem, except that the stress-energy tensor S_{ij} is replaced by its projection, $S_{ij} - \frac{1}{3}S_{kl}g^{kl}g_{ij}$. This ensures that the volume of the fundamental domain, proportional to $\sqrt{\det g}$, is unchanged by arrested Newton flow.

We computed the compression modulus for the multiwall crystal, as this is the crystal with the lowest energy and hence the best candidate to model nuclear matter. As in the previous section, we used the calibration of Gudnason-Speight [11].

The resulting data are plotted in figure 3 and we determine a compression modulus value of $K_0 = 370\,\mathrm{MeV}$, roughly 1/3 of the value $E_0 = 917.3\,\mathrm{MeV}$ for the saturation energy obtained from our model. This result is comparable in magnitude with other theoretical calculations of the compression modulus, and also with the range $250 < K_0 < 315\,\mathrm{MeV}$ determined by a recent survey of experimental data [24].

This result is a significant improvement on values obtained in other Skyrme models. For example, a recent calculation based on the sextic Skyrme model (and also using the multiwall crystal) obtained a value $K_0 = 1169\,\mathrm{MeV}$ and a ratio $K_0/E_0 = 1.28$. We have also carried out a calculation in the standard Skyrme model with massless pions, and obtained a value $K_0/E_0 = 0.973$. Both values are much higher than the value $K_0/E_0 \approx 1/4$ obtained from experiment.

The fact that our value for K_0 is small in comparison with other Skyrme models indicates that the minimum of $E(n_B)/B$ at $n_0 = 0.047\,\mathrm{fm}^{-3}$ is shallow, so energies do not change much as density is varied. This is reminiscent of the fact that the calibration of [11] produces low classical binding energies. It is also consistent with the observation that in other versions of the Skyrme model the multiwall crystal exhibits the smallest variation in energy amongst all crystals as the density is decreased [7]. So our favourable result for the compression modulus can be attributed both to the success of the ω-meson model in producing low binding energies and to particular properties of the multiwall crystal.

JHEP06(2024)116

7 Concluding remarks

In this paper we have constructed crystalline configurations in the ω-meson variant of the Skyrme model and investigated their applications to cold dense nuclear matter. Our construction was based on a new algorithm that combined methods developed in [11] and [7]. It minimizes energy with respect to variations in both the Skyrme field and the period lattice.

Using these new crystals, we have calculated coefficients in the Bethe-Weizsäcker semi-empirical mass formula and the nuclear matter incompressibility coefficient. In both cases we obtained results that are comparable with other theoretical models and with experimental evidence. This is a substantial improvement on previous studies based on other variants of the Skyrme model.

The ω-meson variant of the Skyrme model has also been successful in reproducing binding energies of light nuclei [11]. So this variant of the Skyrme model shows promise as a model of nuclear physics, and is worthy of further study.

Acknowledgments

P. Leask is supported by a Ph.D. studentship from UKRI, Grant No. EP/V520081/1. We would like to thank the organisers of the Solitons (non)Integrability Geometry XI (SIG XI) conference, where this paper was conceptualised.

Open Access. This article is distributed under the terms of the Creative Commons Attribution License (CC-BY4.0), which permits any use, distribution and reproduction in any medium, provided the original author(s) and source are credited.

References

[1] E. Witten, *Global Aspects of Current Algebra*, *Nucl. Phys. B* **223** (1983) 422 [INSPIRE].

[2] E. Witten, *Current Algebra, Baryons, and Quark Confinement*, *Nucl. Phys. B* **223** (1983) 433 [INSPIRE].

[3] T.H.R. Skyrme, *A nonlinear field theory*, *Proc. Roy. Soc. Lond. A* **260** (1961) 127 [INSPIRE].

[4] C. Adam, A. Garcia Martín-Caro, M. Huidobro and A. Wereszczynski, *Skyrme Crystals, Nuclear Matter and Compact Stars*, *Symmetry* **15** (2023) 899 [arXiv:2305.06639] [INSPIRE].

[5] M. Kugler and S. Shtrikman, *A new Skyrmion crystal*, *Phys. Lett. B* **208** (1988) 491 [INSPIRE].

[6] L. Castillejo et al., *Dense Skyrmion systems*, *Nucl. Phys. A* **501** (1989) 801 [INSPIRE].

[7] D. Harland, P. Leask and M. Speight, *Skyrme crystals with massive pions*, *J. Math. Phys.* **64** (2023) 103503 [arXiv:2305.14005] [INSPIRE].

[8] G.S. Adkins and C.R. Nappi, *Stabilization of Chiral Solitons via Vector Mesons*, *Phys. Lett. B* **137** (1984) 251 [INSPIRE].

[9] P. Sutcliffe, *Multi-Skyrmions with Vector Mesons*, *Phys. Rev. D* **79** (2009) 085014 [arXiv:0810.5444] [INSPIRE].

[10] J.M. Speight, *A simple mass-splitting mechanism in the Skyrme model*, *Phys. Lett. B* **781** (2018) 455 [arXiv:1803.11216] [INSPIRE].

JHEP06(2024)116

[11] S.B. Gudnason and J.M. Speight, *Realistic classical binding energies in the ω-Skyrme model*, *JHEP* **07** (2020) 184 [arXiv:2004.12862] [INSPIRE].

[12] P. Leask, *Baby skyrmion crystals stabilized by vector mesons*, arXiv:2403.14810 [INSPIRE].

[13] B.-Y. Park, M. Rho and V. Vento, *Vector mesons and dense Skyrmion matter*, *Nucl. Phys. A* **736** (2004) 129 [hep-ph/0310087] [INSPIRE].

[14] Y.-L. Ma et al., *Dense baryonic matter in the hidden local symmetry approach: Half-skyrmions and nucleon mass*, *Phys. Rev. D* **88** (2013) 014016 [*Erratum ibid.* **88** (2013) 079904] [arXiv:1304.5638] [INSPIRE].

[15] H. Forkel, A.D. Jackson and C. Weiss, *Skyrmions with vector mesons: Stability and the vector limit*, *Nucl. Phys. A* **526** (1991) 453 [INSPIRE].

[16] G. Barriga, M. Torres and A. Vera, *Exact modulated hadronic tubes and layers at finite volume in a cloud of π and ω mesons*, *Nucl. Phys. B* **1001** (2024) 116501 [arXiv:2312.16131] [INSPIRE].

[17] P.-G. Reinhard, M. Bender, W. Nazarewicz and T. Vertse, *From finite nuclei to the nuclear liquid drop: Leptodermous expansion based on the self-consistent mean-field theory*, *Phys. Rev. C* **73** (2006) 014309 [nucl-th/0510039] [INSPIRE].

[18] W.K. Baskerville, *Making nuclei out of the Skyrme crystal*, *Nucl. Phys. A* **596** (1996) 611 [nucl-th/9510047] [INSPIRE].

[19] P. Leask, *Baby Skyrmion crystals*, *Phys. Rev. D* **105** (2022) 025010 [arXiv:2111.02217] [INSPIRE].

[20] C. Naya and P. Sutcliffe, *Skyrmions and clustering in light nuclei*, *Phys. Rev. Lett.* **121** (2018) 232002 [arXiv:1811.02064] [INSPIRE].

[21] N. Ma, C.J. Halcrow and H. Zhang, *Effect of the Coulomb energy on Skyrmions*, *Phys. Rev. C* **99** (2019) 044312 [arXiv:1901.06025] [INSPIRE].

[22] P. Leask, M. Huidobro and A. Wereszczynski, *Generalized skyrmion crystals with applications to neutron stars*, *Phys. Rev. D* **109** (2024) 056013 [arXiv:2306.04533] [INSPIRE].

[23] U. Garg and G. Colò, *The compression-mode giant resonances and nuclear incompressibility*, *Prog. Part. Nucl. Phys.* **101** (2018) 55 [arXiv:1801.03672] [INSPIRE].

[24] J.R. Stone, N.J. Stone and S.A. Moszkowski, *Incompressibility in finite nuclei and nuclear matter*, *Phys. Rev. C* **89** (2014) 044316 [arXiv:1404.0744] [INSPIRE].

JHEP06(2024)116